Appendix A.49:

Bracken St – CPT 59661

Table 1: Site Description for Bracken St (CPT 59661).

Attribute	Yes/No			Description/Date	Symbol in Figure 1
	10-m Buffer	20-m Buffer	50-m Buffer		
Near a body of surface water or other free face features?	No	No	No	The center of the site is ~115 m to the SE from the Avon River (the free-face height is ~1 m).	NA
Lateral spreading observed during the CES?	No	No	Yes	Ground cracks 10-50 mm in width appear to be a local feature and are present in the N portion of the 20-m buffer and ground cracks up to 100-mm wide (also a local feature) are in all quadrants of the 50-m buffer. The mapping team[1] observed lateral spreading at the property in the SE quadrant of the 50-m buffer and measured the width of ground cracks at the property as 200-300 mm.	NA
Nearby buildings or structures?	Yes	Yes	Yes	Building coverage of the 10-, 20-, and 50-m buffers is 46, 28, and 25%, respectively. Buildings are in all quadrants of all buffers.	White Fill + Brown Outline
Sloping land?	No	No	No	Flat land, residential area	NA
Step changes in the ground surface?	No	No	No	NA	NA
Retaining walls?	No	No	No	NA	NA
Vegetation?	Yes	Yes	Yes	Trees and bushes cover 18, 28, and 30% of the 10-, 20-, and 50-m buffers, respectively. They are in the NW, NE, and SE quadrants of the 10-m buffer and all quadrants of the 20-m and 50-m buffers.	White Fill + Green Outline
Anthropogenic changes to the site between the LiDAR surveys?	Yes	Yes	Yes	Vegetation removal in the SW quadrant of the 50-m buffer between Dec 2004 and Mar 2009. Building addition in the SW quadrant of the 50-m buffer between Jan 2006 and Mar 2009. All buildings within the 50-m buffer were removed between Apr 2012 and July 2015.	Building Addition/ Removal: Orange Crossline
Other important factors?	No	Yes	Yes	Low-motor-vehicle-volume, two-way road (Bracken St) occupies 7% and 16% of the 20-m and 50-m buffers, respectively. It runs through their NE and SE quadrants in the N-S direction.	Road: White Fill + Gray Outline

Note: Buffer is the area within a circle of a specified radius with CPT investigations done at its center (172.663966°, -43.520893°).

[1] Canterbury Geotechnical Database. (2012). "Observed Ground Crack Locations", Map Layer CGD0400 - 23 July 2012, retrieved July 09, 2018 from https://canterburygeotechnicaldatabase.projectorbit.com/

Figure 1: Site plan with areas where ejecta-induced settlement is considered.

Note 1: Patch A (outlined in red) in the free field was selected for settlement assessment as an area free of vegetation and structures. Other important factors considered in the patch selection process were its proximity to a CPT, a property subjected to addition and/or demolition of a structure, front yard/backyard alterations (e.g., ploughing, rubble, scrap), and aerial distribution of sediment ejecta. The LiDAR-based settlement analyses were not performed for any earthquake event due to the uncertainties explained in Table 2.

Table 2: LiDAR flight error adjustments, global adjustments for the difference between average LiDAR point elevations and benchmark survey elevations, and vertical tectonic movement adjustments.

	Adjustments (mm)		
Earthquake Event(s)	LiDAR Flight Error	Global Offset[2]	Tectonic Vertical Movement
Sep-10	-100	-3	0
Feb-11	+100	16	-100
Jun-11	0	38	-40
Dec-11	-50	-65	0
CES	-50	-14	-140
Any LiDAR survey affected by ejecta?			Yes*

Notes: The negative sign indicates the subtraction from the ground surface subsidence, while the positive sign indicates the addition to the ground surface subsidence; * Ejecta on the road were not removed at the time of the Sep 2010 and March 2011 LiDAR surveys; It is most likely that ejecta were not removed from Patch A at the time of the Sep 2010 LiDAR survey; Ejecta were not removed after the June 2011 earthquake but the Dec 2011 earthquake.

Table 3: LiDAR Measurement Error for Patch A.

Surveys	Buffer	Area Averaged Difference Indicating Repeat Measurement Error (mm)	σ*$_{\text{individual LiDAR points}}$ (mm)	%Reduction in σ due to Area Averaging of LiDAR Points
Post Feb 2011: Mar 2011 and May 2011	10-m	NA	59	[ND,ND]
	20-m	ND		
	50-m	ND		
Post Dec 2011: Feb 2012 and Oct 2015	10-m	NA	70	[ND,ND]
	20-m	ND		
	50-m	ND		

*Standard deviation; NA = Not available; ND = Not determined.

[2] Russell, J., & van Ballegooy, S. (2015). *Canterbury Earthquake Sequence: Increased liquefaction vulnerability assessment methodology*. New Zealand: Tonkin & Taylor Ltd.

Table 4: Ground surface subsidence adjustments due to LiDAR measurement error for Patch A.

Earthquake Event(s)	$\sigma_{\text{pre-EQ LiDAR survey}}$ (mm)	$\sigma_{\text{post-EQ LiDAR survey}}$ (mm)	σ_{total} (mm)	Area Average Adjusted σ (mm) **
Sep-10	158	56	134	ND
Feb-11	56	59	59	ND
Jun-11	59	61	62	ND
Dec-11	61	70	87	ND
CES	158	70	124	ND

**Based on the highest %Reduction in Table 3; ND = Not determined.

Table 5: Raw liquefaction-related ground surface subsidence using original LiDAR points for Patch A.

	Average Ground Surface Subsidence (mm)		
Earthquake Event(s)	10-m Buffer	20-m Buffer	50-m Buffer
Sep-10	NA	ND	ND
Feb-11	NA	ND	ND
Jun-11	NA	ND	ND
Dec-11	NA	ND	ND
CES	NA	ND	ND

Table 6: Corrected liquefaction-related ground surface subsidence using original LiDAR points for Patch A with the calculated adjustments in Table 2.

	Average Calculated Ground Surface Subsidence (mm)		
Earthquake Event(s)	10-m Buffer	20-m Buffer	50-m Buffer
Sep-10	NA	ND	ND
Feb-11	NA	ND	ND
Jun-11	NA	ND	ND
Dec-11	NA	ND	ND
CES	NA	ND	ND

Notes: Plus/minus values are same as those in Table 4a, but rounded to the nearest 25 mm; Positive overall values indicate ground surface subsidence, while negative overall values indicate ground surface uplift.

Table 7: Corrected liquefaction-related ground surface subsidence for Patch A using LiDAR DEMs.

	Estimated Ground Surface Subsidence (mm)								
	10-m Buffer			20-m Buffer			50-m Buffer		
Earthquake Event(s)	16th %ile	50th %ile	84th %ile	16th %ile	50th %ile	84th %ile	16th %ile	50th %ile	84th %ile
Sep-10	NA	NA	NA	ND	ND	ND	ND	ND	ND
Feb-11	NA	NA	NA	ND	ND	ND	ND	ND	ND
Jun-11	NA	NA	NA	ND	ND	ND	ND	ND	ND
Dec-11	NA	NA	NA	ND	ND	ND	ND	ND	ND
CES	NA	NA	NA	ND	ND	ND	ND	ND	ND

Note: These percentiles are not the exact statistical measures; they indicate the spatial variability of ground surface subsidence.

Table 8: Ejecta-Induced settlement for the top 20 m of the soil profile for Patch A (50-m buffer for the 50th %ile PGA, P_L=50%, and C_{FC}=0.13 using BI-2014, ZRB-2002, and I_C cutoff of 2.6.

Earthquake Event(s)	M_W	PGA (g)	Depth to Groundwater (m)	S_T (mm)	S_{V1D} (mm)	$S_{E,L}$ (mm)
Sep-10	7.1	0.21	1.5	ND	29±20	ND
Feb-11	6.2	0.47	1.5	ND	139±50	ND
Jun-11	6.2	0.27	1.5	ND	44±25	ND
Dec-11	6.1	0.26	1.5	ND	34±50	ND

Notes: S_T = Total settlement (Table 6); S_{V1D} = Average vertical settlement due to volumetric compression using Boulanger and Idriss (2014) (BI-2014), Zhang et al. (2002) (ZRB-2002) procedures and de Greef and Lengkeek (2018) thin-layer correction; $S_{E,L}$ = Ejecta-induced settlement as the difference between the LiDAR-based S_T and S_{V1D}.

Note 2: The uncertainty for volumetric settlement was derived based on the sensitivity of volumetric settlement to PGA, C_{FC}, and P_L for each earthquake event for VsVp 57203 *Shirley Intermediate School* and CC LIQ 1 – CPT 5586 – *Vivian St* sites. Taking the 50th percentile as the baseline case, the minimum and maximum values corresponding to the difference between the 25th percentile and the 50th percentile and the 75th percentile and the 50th percentile were determined. The arithmetic mean of the range of the minimum and maximum difference was evaluated for each patch at the two sites. The maximum arithmetic mean for each earthquake event was rounded to the nearest five and used as the uncertainty value. Accordingly, the 1-D volumetric settlement uncertainties of ±20, ±50, ±25, and ±50 mm for the Sep-10, Feb-11, Jun-11, and Dec-11 earthquake events, respectively, were used for all sites in this study.

Table 9: Coverage area and height of ejecta estimates for Patch A (50-m buffer) using photographs.

EQ Event	$H_{E,thick1}$ (mm)	$A_{E,thick1}$ (m^2)	$H_{E,thick2}$ (mm)	$A_{E,thick2}$ (m^2)	$H_{E,thin1}$ (mm)	$A_{E,thin1}$ (m^2)	$H_{E,thin2}$ (mm)	$A_{E,thin2}$ (m^2)	A_T (m^2)
Sep-10	80-120	29.1	30-60	29.4	20-40	1.8	0	0	103
Feb-11	120-160	44.0	70-100	11.6	30-50	4.3	20-40	8.3	103
Jun-11	90-130	12.1	50-80	8.2	40-60	3.5	20-50	20.5	103
Dec-11	70-100	13.0	40-60	11.6	20-40	0.9	5-10	2.1	103

Notes: $A_{E,thin/thick}$ = Coverage area of thin/thick ejecta layers; $H_{E,thin/thick}$ = Lower-upper estimate of height of thin/thick ejecta layers; A_T= Total assessment area of a buffer being considered.

Note 3: The values in Table 9 correspond to the coverage area of ejecta outlined in aerial photographs (Figures 37-40) and the lower and upper estimates of ejecta height based on geometrical approximations (Figures 41 and 42), ground photographs, and EQC LDAT property inspection reports (e.g., Figures 43 and 44). The ejecta-induced settlement using photographs and engineering judgment, $S_{E,P}$, is estimated as

$$S_{E,P} = \frac{\sum_{i=1}^{a} A_{E,thick,i} * H_{E,thick,i} + \sum_{j=1}^{b} A_{E,thin,j} * H_{E,thin,j}}{A_T} = \frac{\sum_{i=1}^{a} V_{E,thick,i} + \sum_{j=1}^{b} V_{E,thin,j}}{A_T}$$

where

- $A_{E,thick,i}$ and $H_{E,thick,i}$ are the area and the height of a thick ejecta layer, respectively;
- $A_{E,thin,j}$ and $H_{E,thin,j}$ are the area and the height of a thin ejecta layer, respectively;
- A_T is the total assessment area for a buffer being considered (Figure 1).

Table 10: Ejecta-induced settlement estimates for Patch A based on photographs.

Earthquake Event	Patch A (50-m buffer)	
	$S_{E,P,lower}$ (mm)	$S_{E,P,upper}$ (mm)
Sep-10	32	52
Feb-11	62	85
Jun-11	20	34
Dec-11	14	20

Note: $S_{E,P,lower}$ and $S_{E,P,upper}$ correspond to lower and upper estimates of $S_{E,P}$, respectively.

Table 11: Best final estimates of ejecta-induced settlement for Patch A.

EQ Event	Patch A (50-m buffer)		
	$S_{E,L}$ (mm)	$S_{E,P}$ (mm)	$S_{E,final}$ (mm)
Sep-10	ND	42±10	40±10
Feb-11	ND	74±11	75±10
Jun-11	ND	27±7	25±5
Dec-11	ND	17±3	15±5

Notes: $S_{E,L}$ = Ejecta-induced settlement based on LiDAR data reported in Table 8; $S_{E,P}$ = Median ejecta-induced settlement for the range of values reported in Table 10; $S_{E,final}$ = Best final estimate of ejecta-induced settlement rounded to the nearest 5 mm; Final plus/minus values are also rounded to the nearest 5 mm; ND = Not determined.

Note 4:

- $S_{E,final}$ for Patch A is based solely on $S_{E,P}$ for all earthquake events. Please see Table 2 for the explanation.
- The Bracken St site is in the apparent zone of higher ground surface subsidence for the Sep-10 EQ and the apparent zone of lower ground surface subsidence for the Feb-11 EQ (i.e., the underestimate of the ground surface elevation by the Sep-10 LiDAR survey). The site is in the zone of accurate LPI prediction of liquefaction severity for the Sep-10 and Feb-11 EQs (Maurer et al. 2014[3]). The LDAT inspection report and ground photographs from July 2011 and the inspection report from Oct 2010 are available for the property with Patch A. The height of ejecta from the Jun-11 EQ was measured as ~300 mm. Ejecta within Patch A was also documented by Quigley et al. (2013)[4]. The depth of ejecta in the shallow trench from Apr 2012 was ~100 mm for the Jun-11 EQ and ~100 mm for the Dec-11 EQ.

<u>**Summary 1**</u>**:**

The best estimate of the ejecta-induced free-field ground settlement at the Bracken St site for the SEP 2010, FEB 2011, JUN 2011, and DEC 2011 earthquake is 40±10 mm, 75±10 mm, 25±5 mm, and 15±5 mm, respectively.

[3] Maurer, B. W., Green, R. A., Cubrinovski, M., & Bradley, B. A. (2014). Evaluation of the Liquefaction Potential Index for Assessing Liquefaction Hazard in Christchurch, New Zealand. *Journal of Geotechnical and Geoenvironmental Engineering*, 140(7), 04014032-1-11. doi:10.1061/(asce)gt.1943-5606.0001117

[4] Quigley, M., Bastin, M., and Bradley, B. (2013). Recurrent liquefaction in Christchurch, New Zealand, during the Canterbury earthquake sequence. *Geological Society of America Geology, 41*(4), p. 419-422. doi: 10.1130/G33944.1

Figure 2: Location of the site.

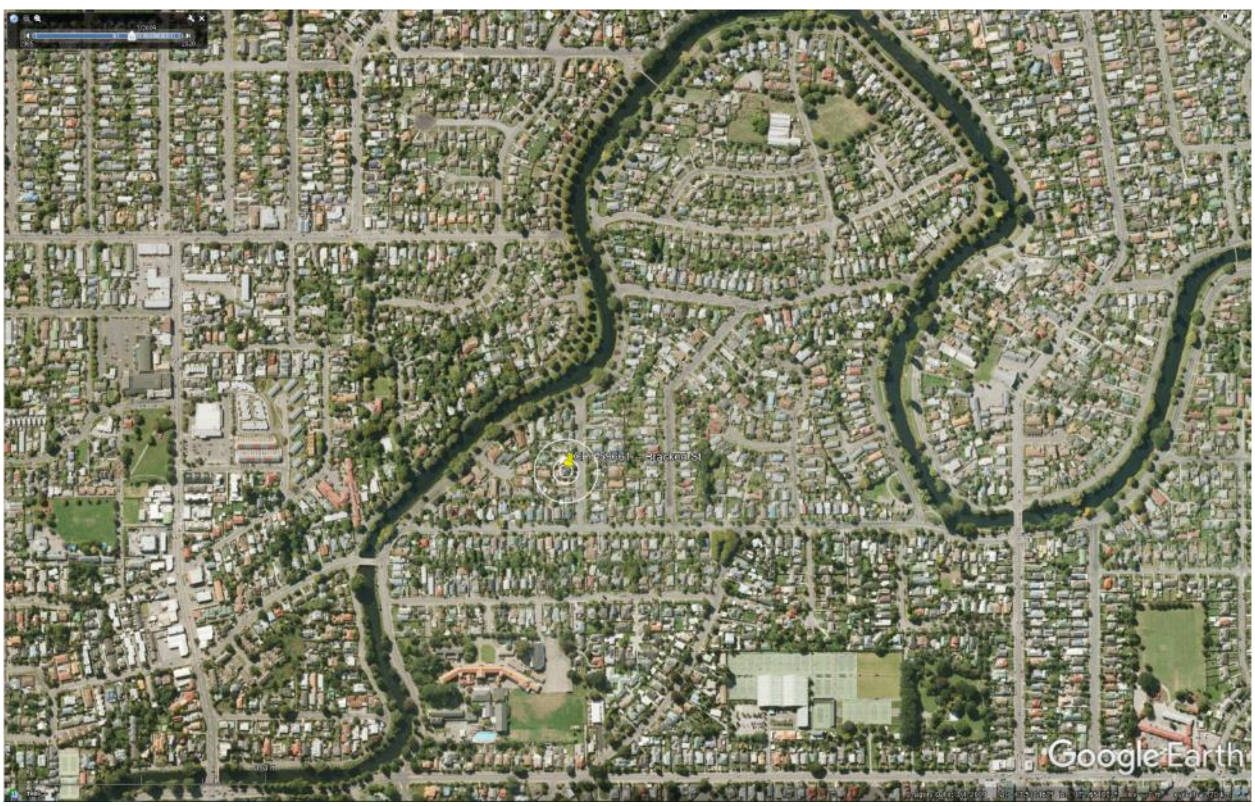

Figure 3: Position of the site relative to nearby buildings, vegetation, and free-face features.

Figure 4: Street view of the flat land.

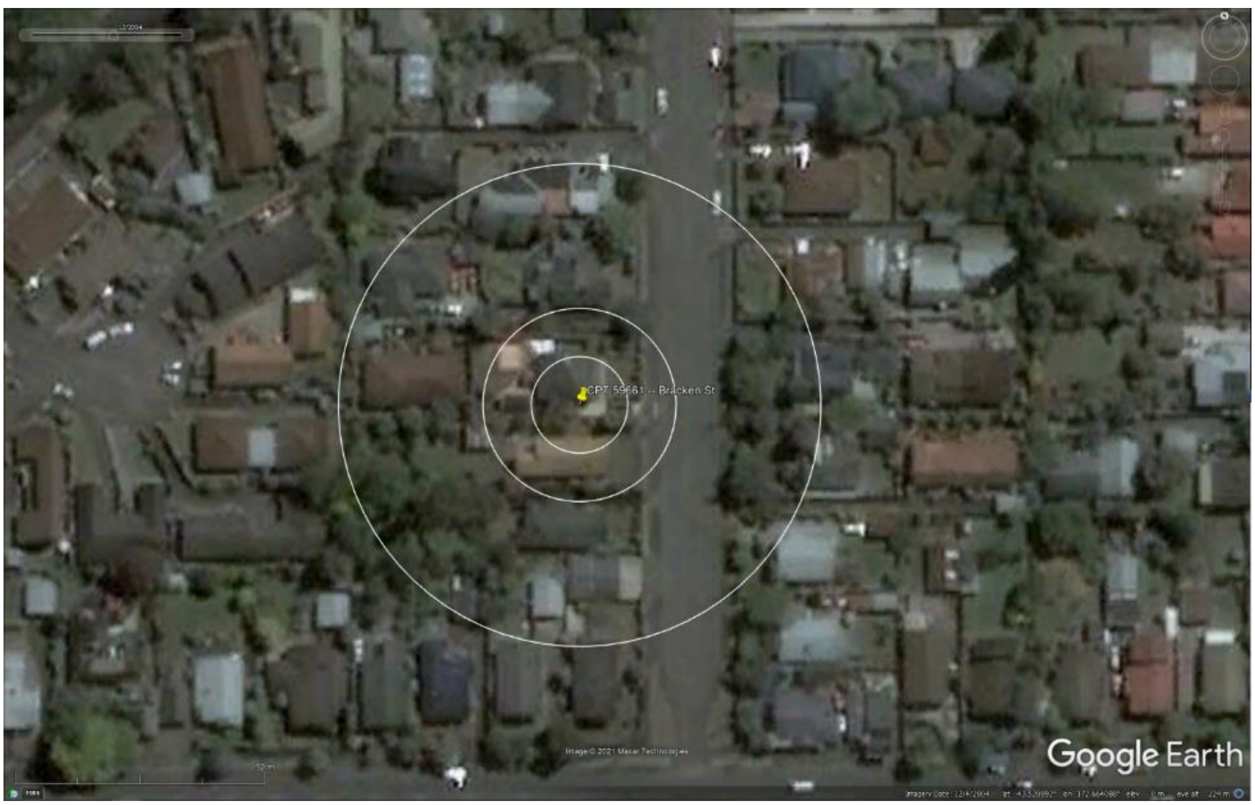

Figure 5: Satellite image of the site taken in Dec 2004.

Figure 6: Satellite image of the site taken in Jan 2006.

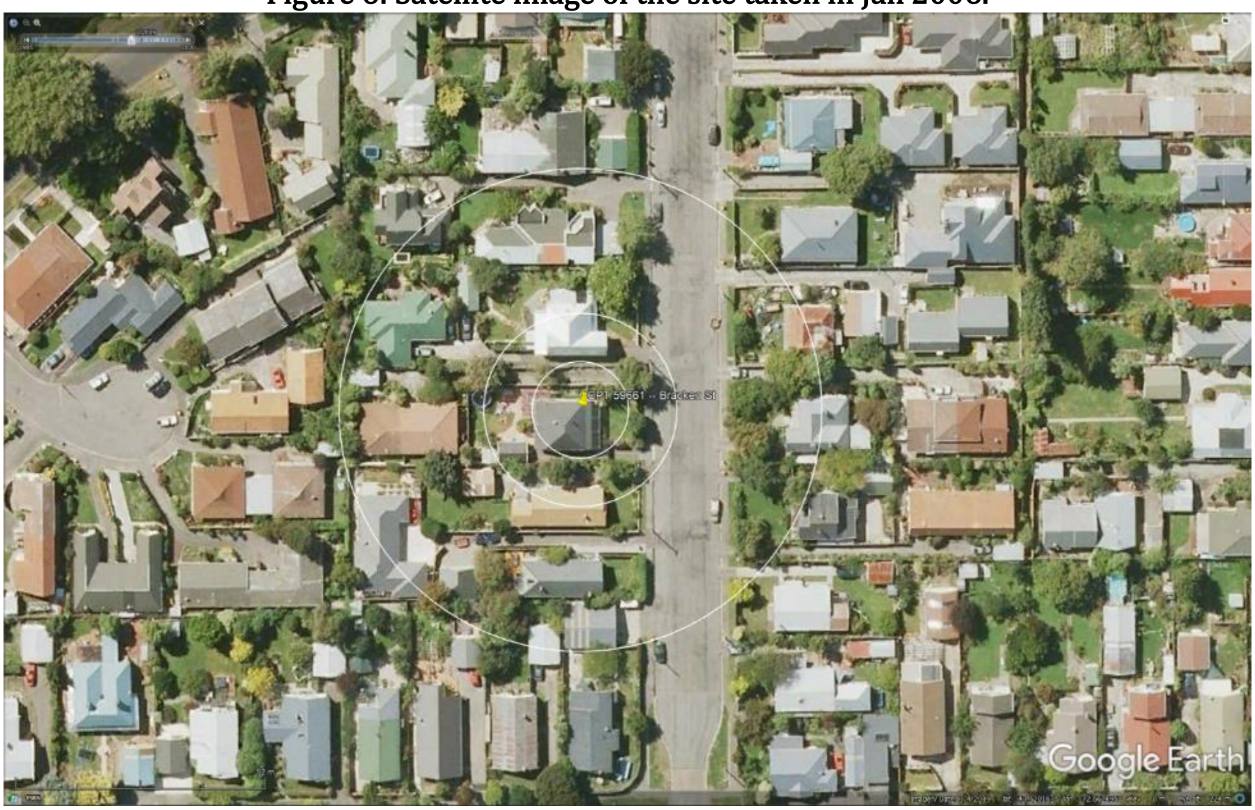

Figure 7: Satellite image of the site taken in Mar 2009.

Figure 8: Satellite image of the site taken on Sep 3, 2010.

Figure 9: Satellite image of the site taken on Sep 5, 2010.

Figure 10: Satellite image of the site taken on Feb 7, 2011.

Figure 11: Satellite image of the site taken on Feb 23, 2011.

Figure 12: Satellite image of the site taken on Feb 26, 2011.

Figure 13: Satellite image of the site taken on Mar 28, 2011.

Figure 14: Satellite image of the site taken in Apr 2012.

Figure 15: Satellite image of the site taken in Jul 2015.

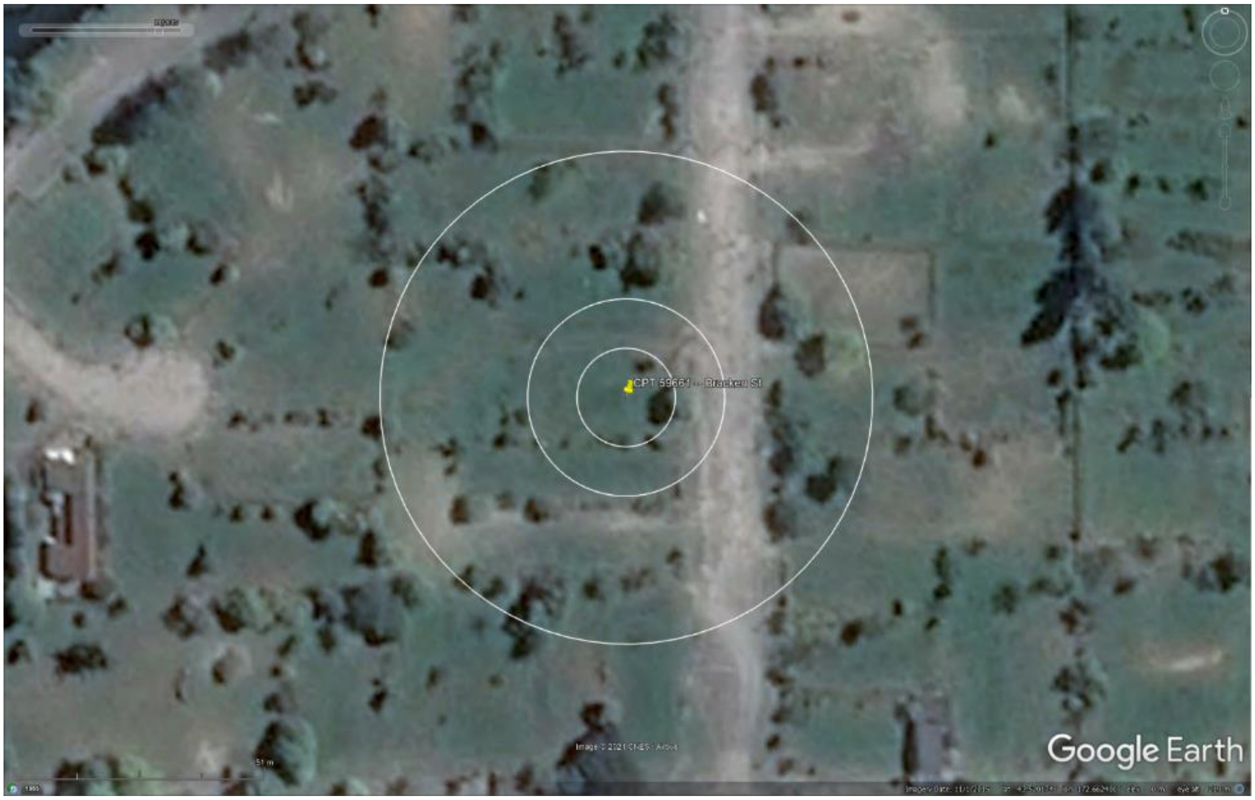

Figure 16: Satellite image of the site taken in Nov 2015.

Figure 17: Aerial photograph of the site taken on Sep 4, 2010.

Figure 18: Aerial photograph of the site taken on Feb 24, 2011.

Figure 19: Aerial photograph of the site taken on June 14-15, 2011.

Figure 20: Aerial photograph of the site taken on June 16, 2011.

Figure 21: Aerial photograph of the site taken on Dec 24, 2011.

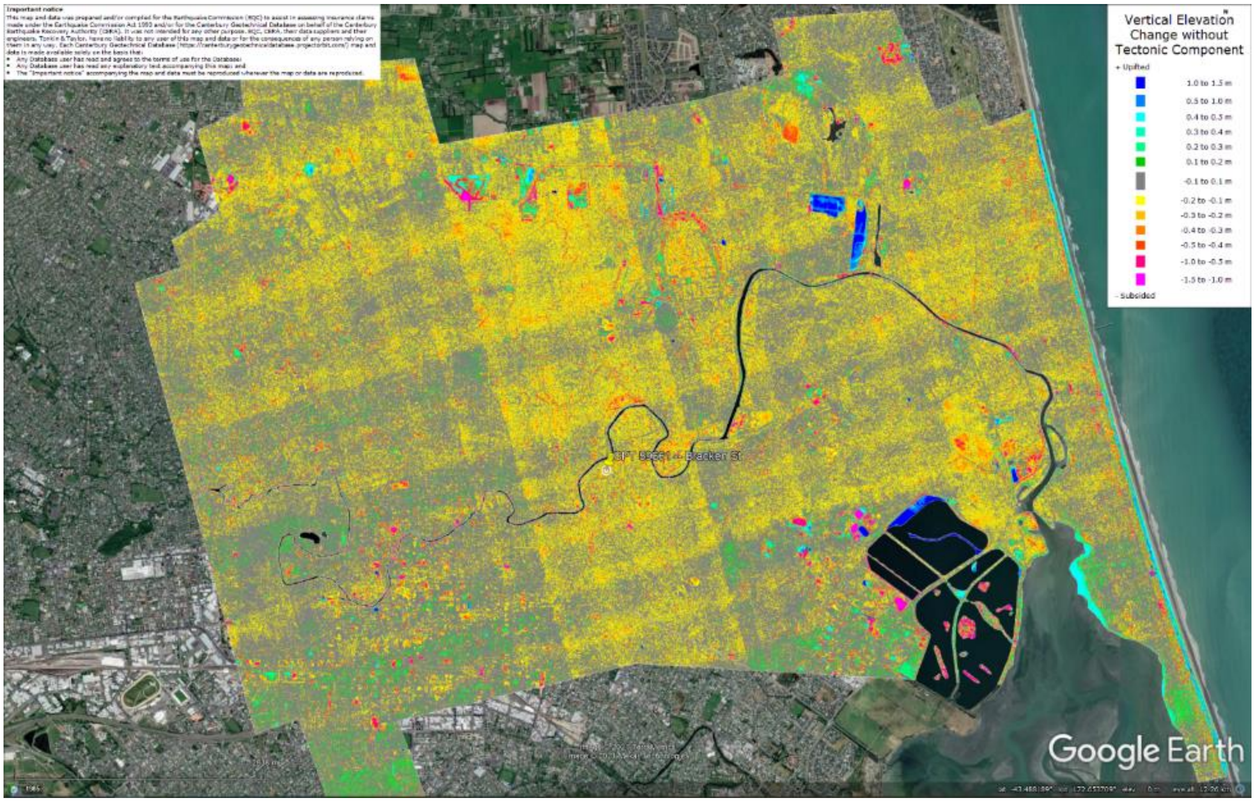

Figure 22: Vertical Ground Movements (Surface – Tectonic) for Sep 2010 Earthquake – the site is in the apparent zone of overestimated ground surface subsidence (i.e., Sep 2010 flight error zone).

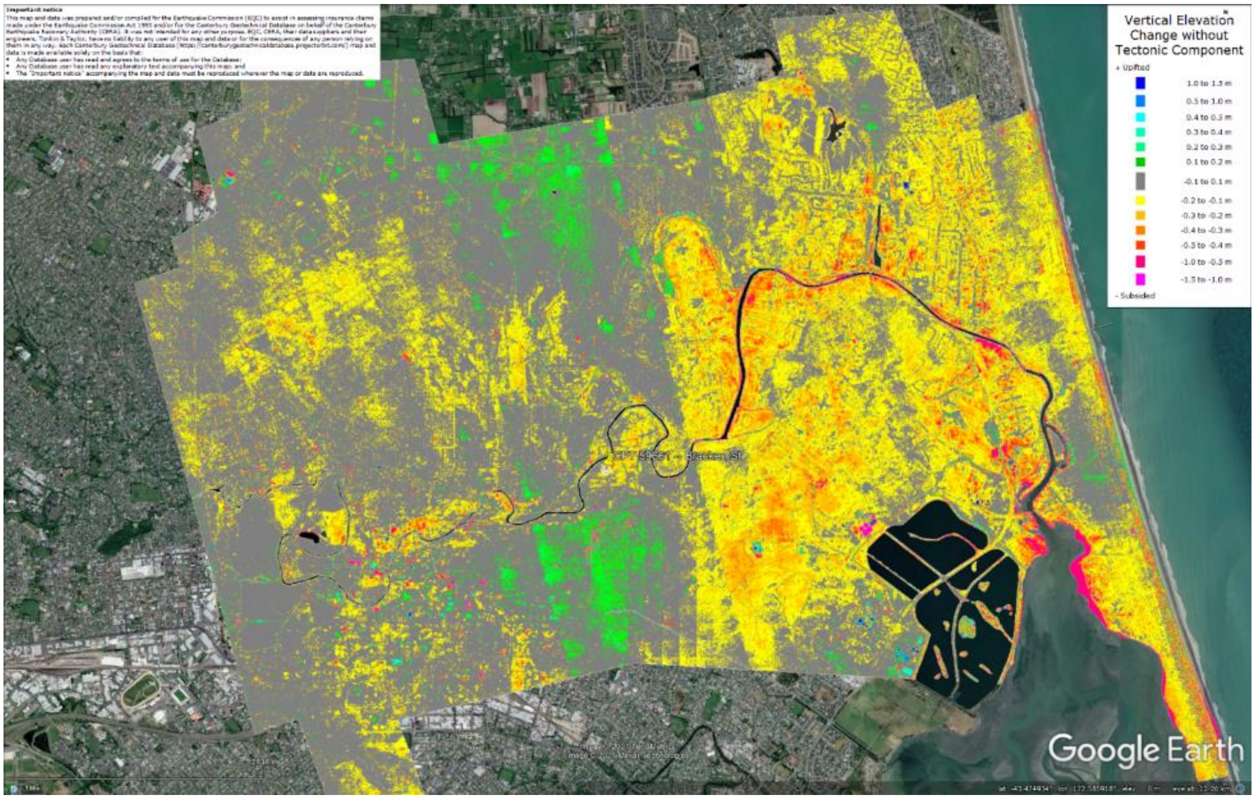

Figure 23: Vertical Ground Movements (Surface – Tectonic) for Feb 2011 Earthquake – the site is in the apparent zone of underestimated ground surface subsidence (i.e., Sep 2010 flight error zone).

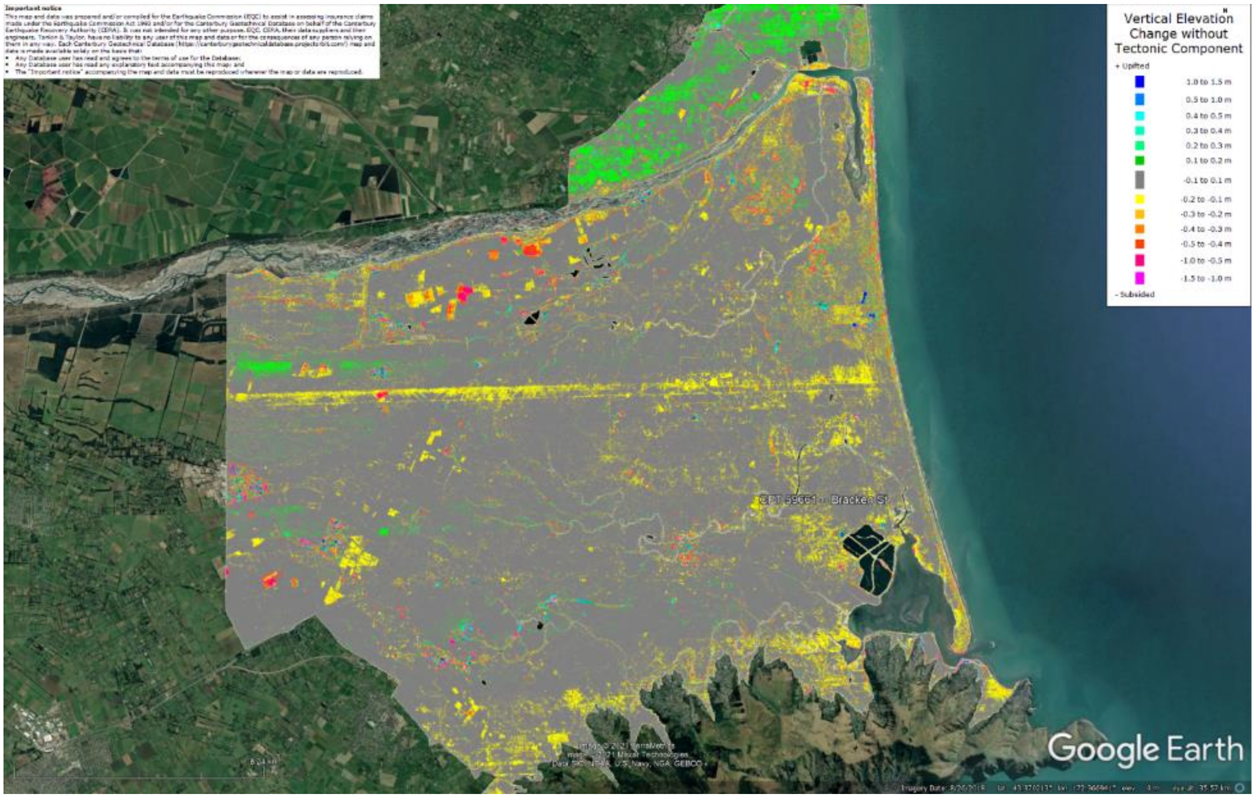

Figure 24: Vertical Ground Movements (Surface – Tectonic) for June 2011 Earthquake – the site is not in the apparent zone of overestimated ground surface subsidence.

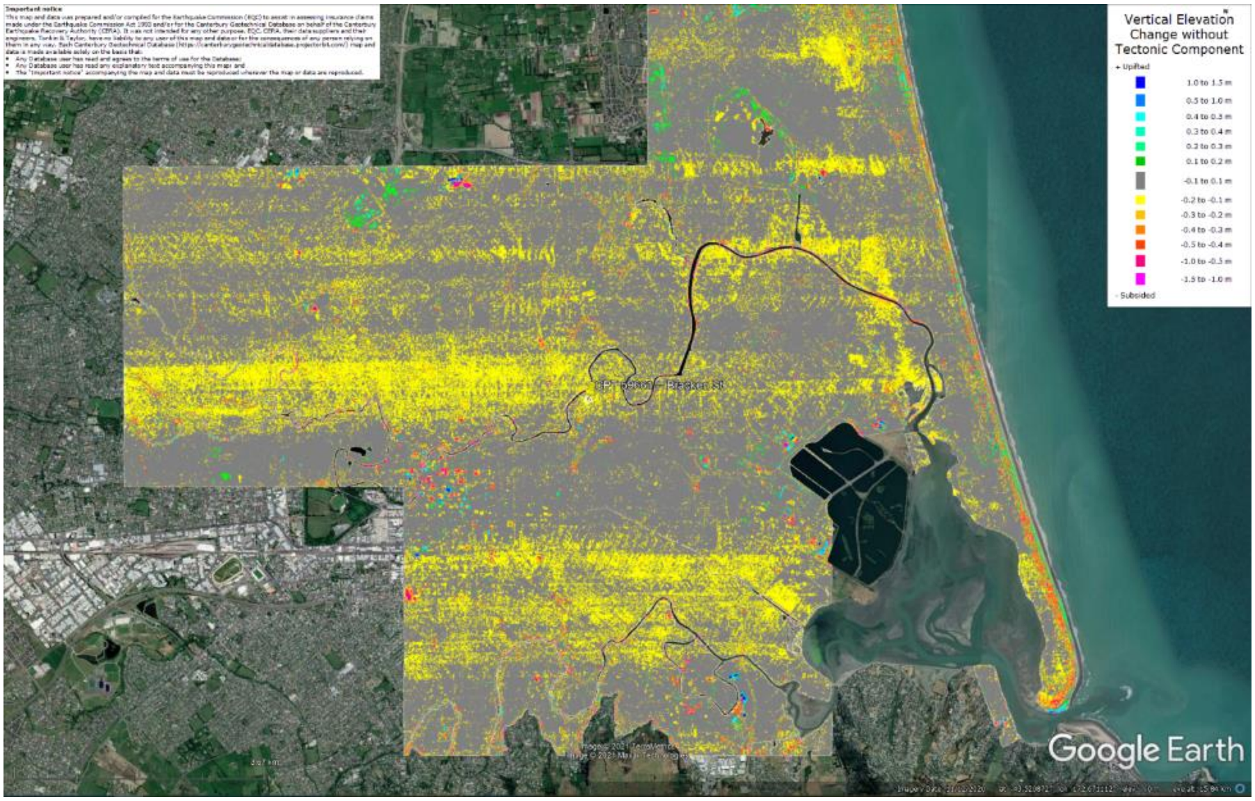

Figure 25: Vertical Ground Movements (Surface – Tectonic) for Dec 2011 Earthquake – the site is in the apparent zone of overestimated ground surface subsidence (i.e., Feb 2012 LiDAR flight band error).

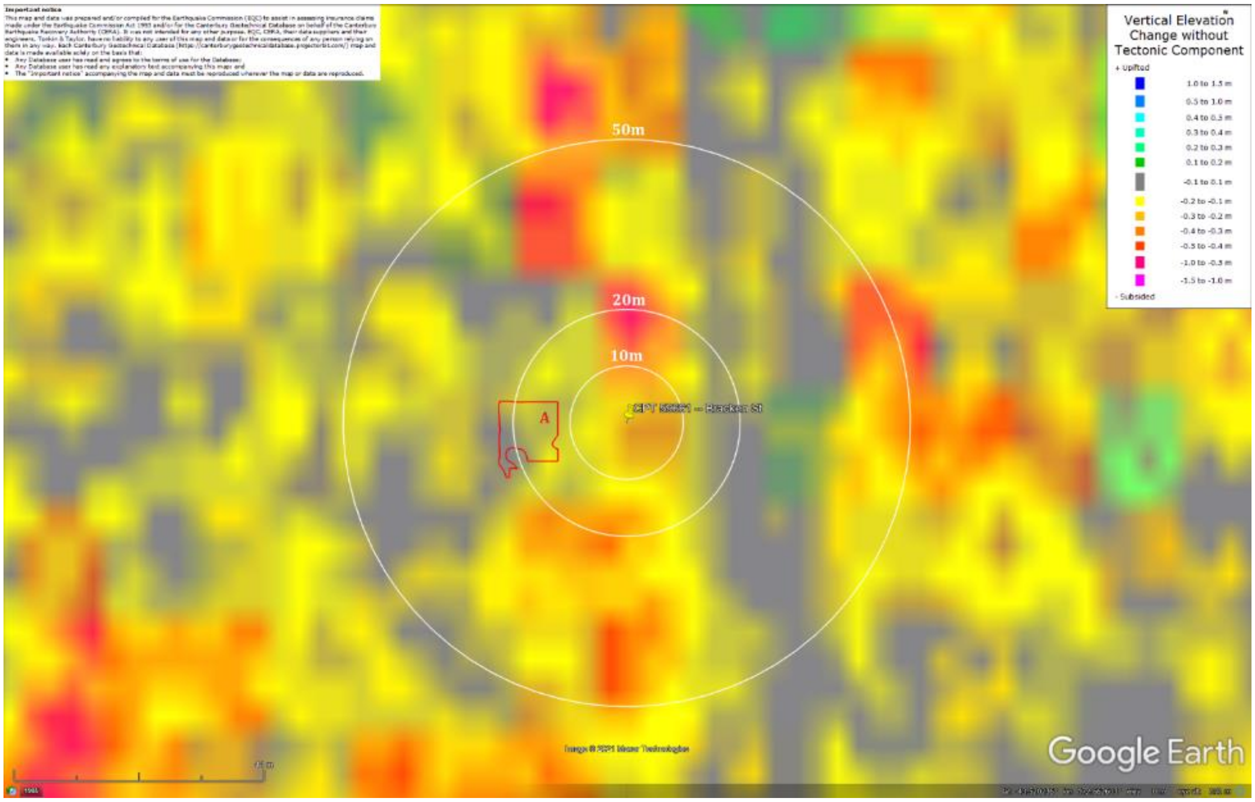

Figure 26: Ground surface subsidence without tectonic component for Sep 2010 Earthquake according to the LiDAR DEM.

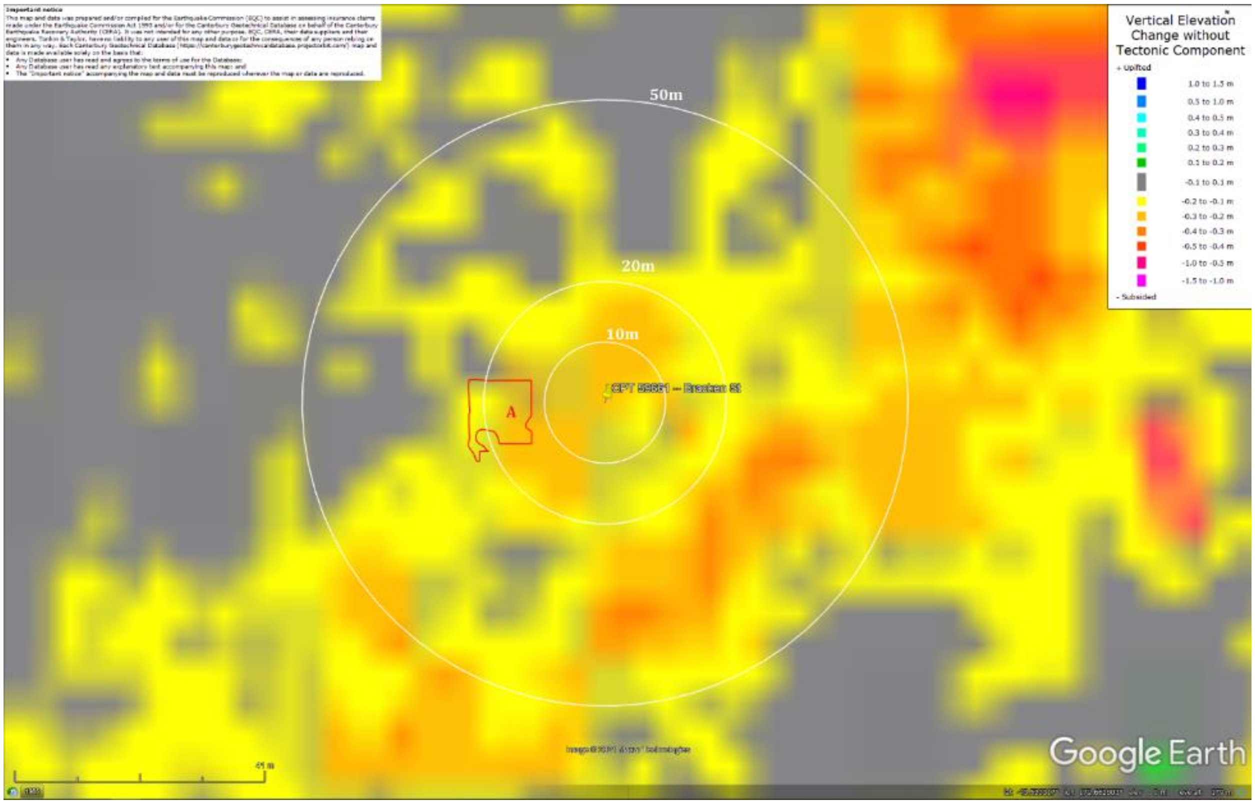

Figure 27: Ground surface subsidence without tectonic component for Feb 2011 Earthquake according to the LiDAR DEM.

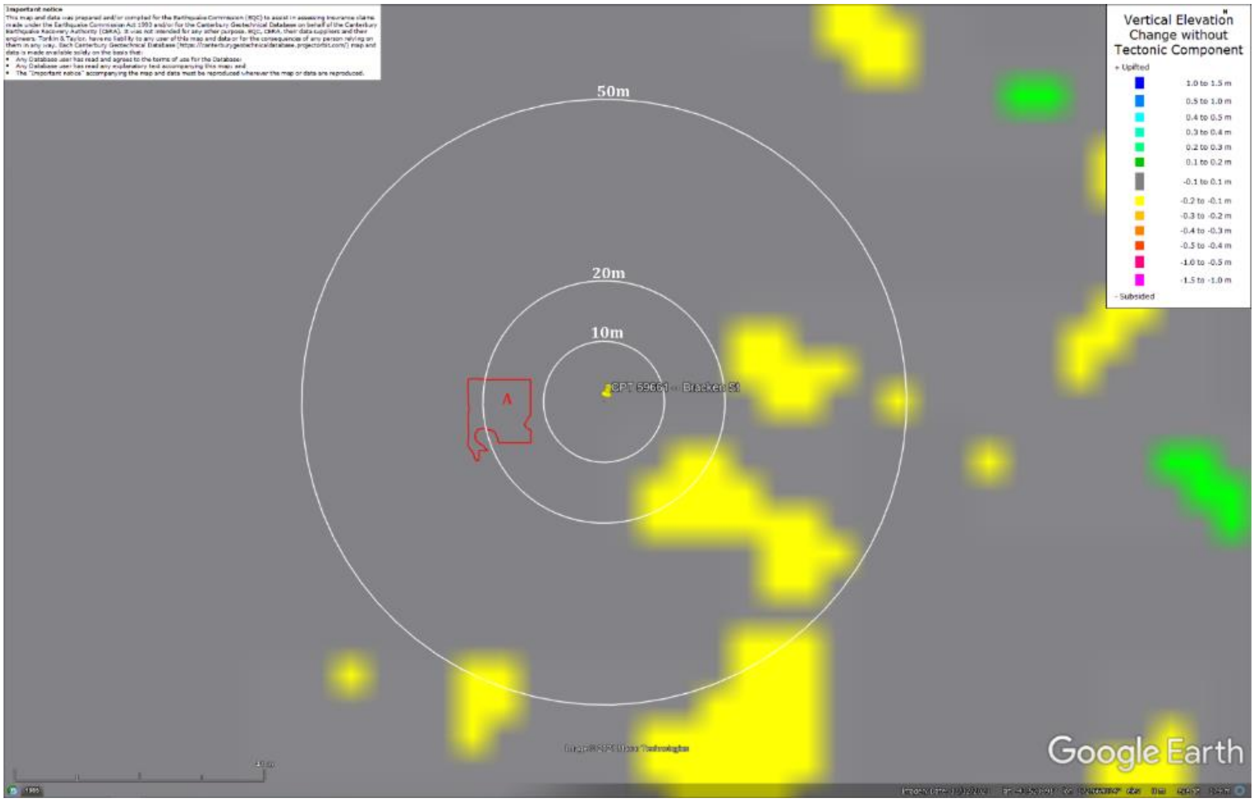

Figure 28: Ground surface subsidence without tectonic component for June 2011 Earthquake according to the LiDAR DEM.

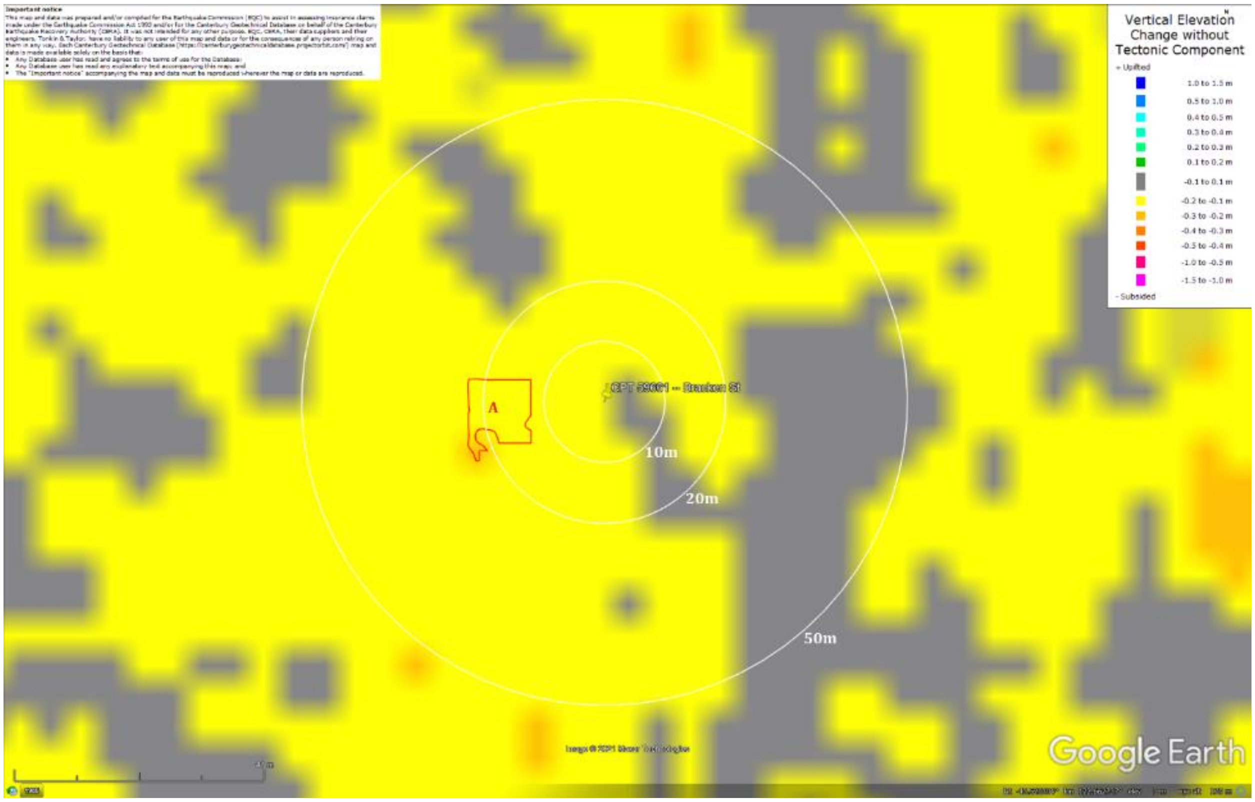

Figure 29: Ground surface subsidence without tectonic component for Dec 2011 Earthquake according to the LiDAR DEM.

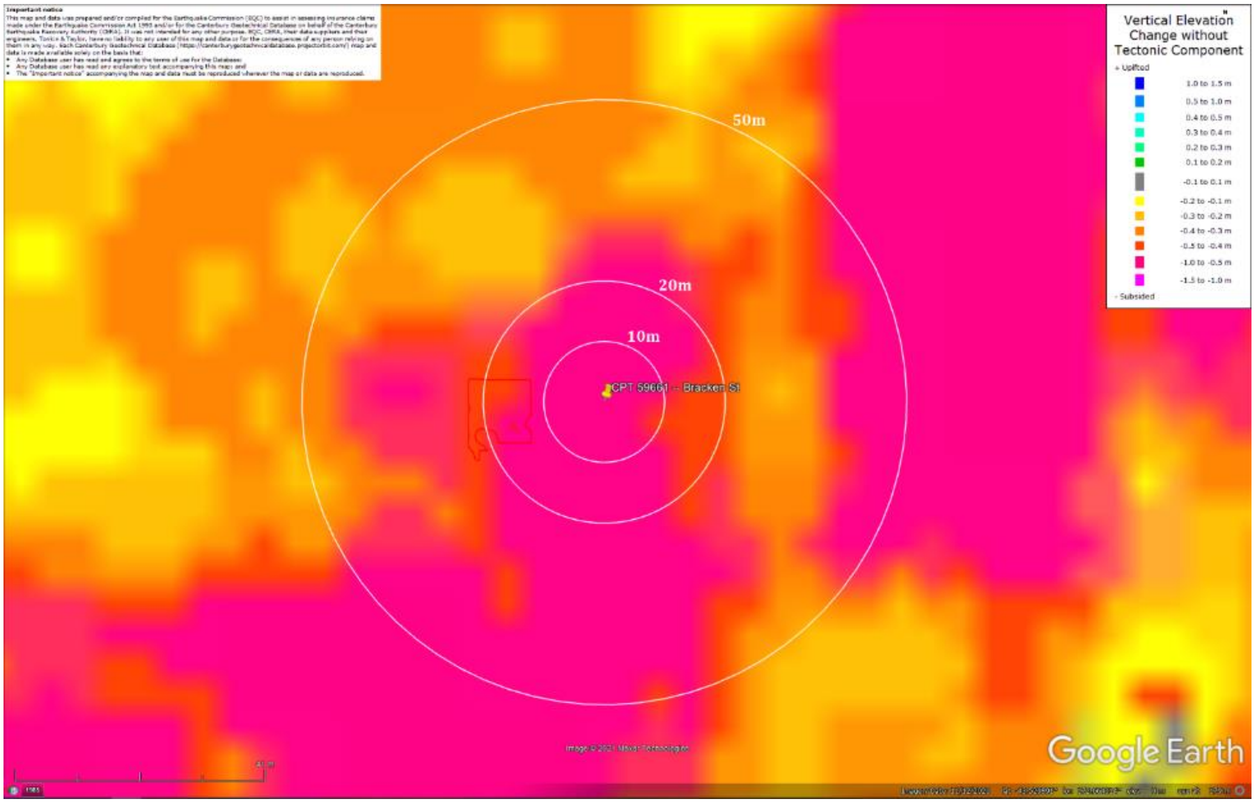

Figure 30: Ground surface subsidence without tectonic component for Canterbury Earthquake Sequence according to the LiDAR DEM.

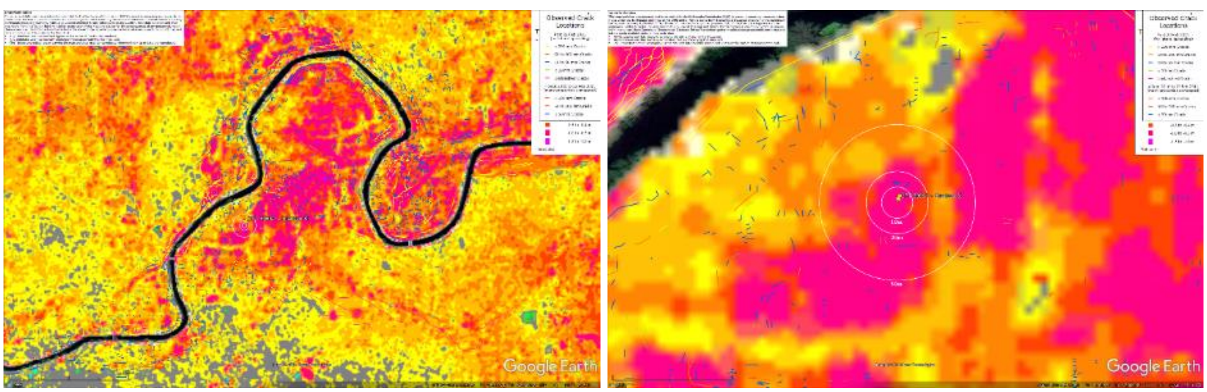

Figure 31: Lateral spreading was observed for the SE quadrant of the 50-m property for the Feb 2011 Earthquake.

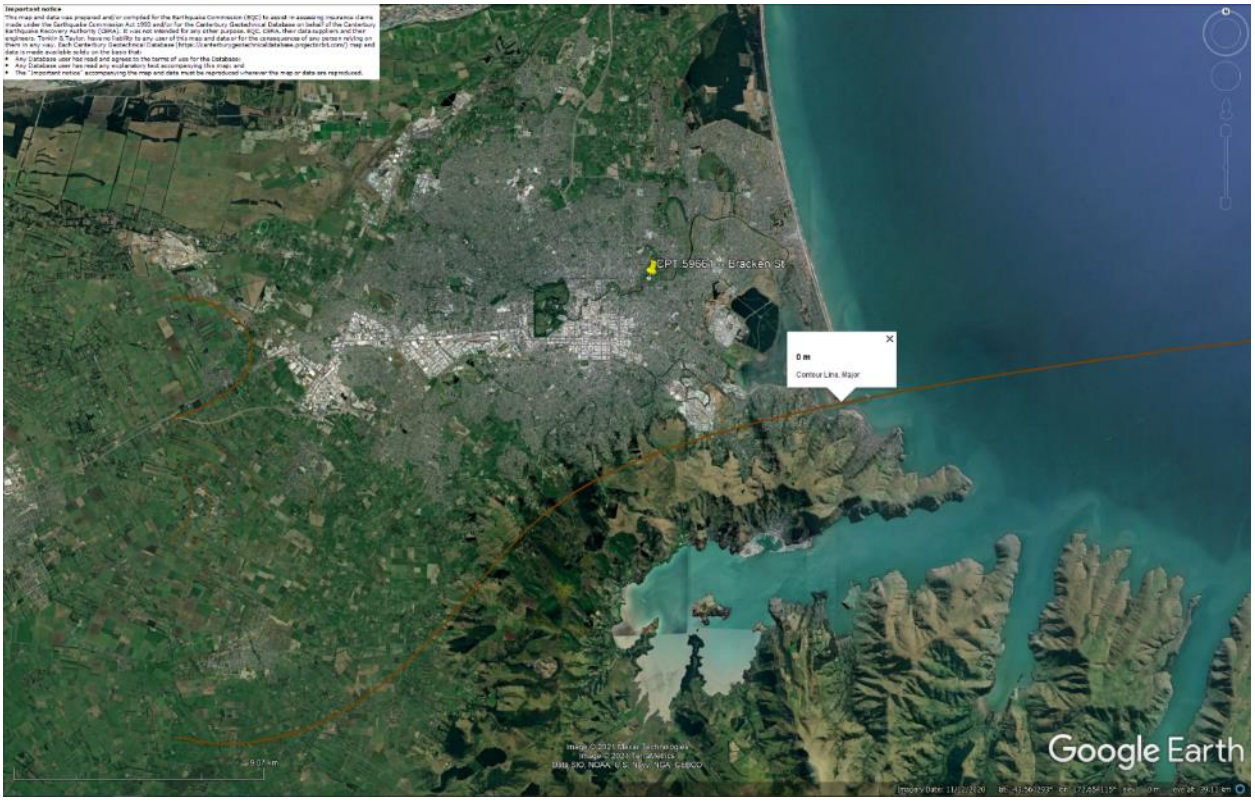

Figure 32: Vertical tectonic movements for Sep 2010 Earthquake.

Figure 33: Vertical tectonic movements for Feb 2011 Earthquake.

Figure 34: Vertical tectonic movements for June 2011 Earthquake.

Figure 35: Vertical tectonic movements for Dec 2011 Earthquake.

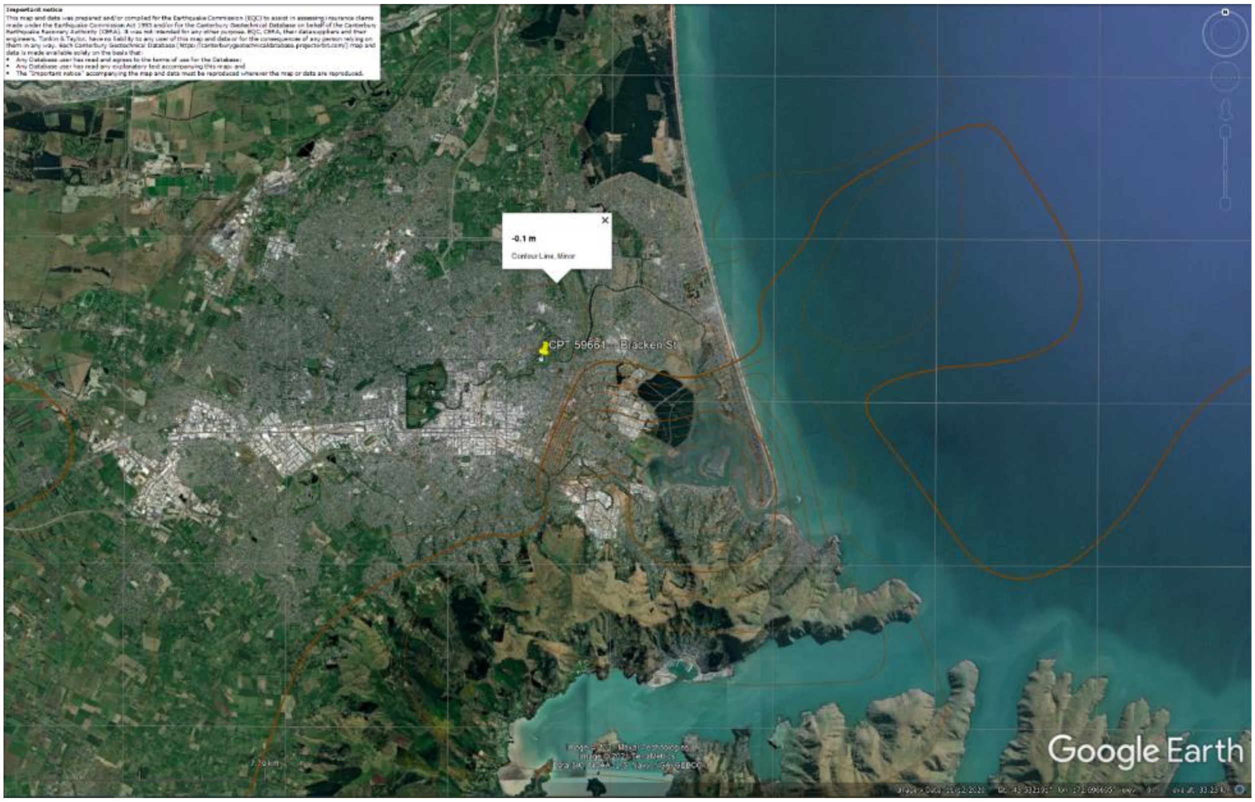

Figure 36: Vertical tectonic movements for Canterbury Earthquake Sequence.

Figure 37: Aerial photograph showing the ejecta outline at the site for Sep-10 EQ.

Figure 38: Aerial photograph showing the ejecta outline at the site for Feb-11 EQ.

Figure 39: Aerial photograph acquired on 16 Jun 2011 showing the ejecta outline at the site for Jun-11 EQ.

Figure 40: Aerial photograph showing the ejecta outline at the site for Dec-11 EQ.

Figure 2. A–F: Field photographs (looking southwest) of sand blows at study site following the (A) Darfield M_L 7.1 earthquake, (B) 22 February 2011 M_L 6.3, 5.8, and 5.9 earthquakes, (C) 16 April 2011 M_L 5.5 earthquake, (D) 13 June 2011-a M_L 5.6 earthquake, (E) 13 June 2011-b M_L 6.4 earthquake, and (F) 23 December 2011 M_L 5.8 and 6.0 earthquakes. All photos were taken from same location within 3 h of last inducing earthquake. G: Distinct liquefaction ejecta units in sand blow stratigraphy. Arrows and nails denote silt drapes. Cross-bedding as sketched. Location of photographed portion of trench location shown in F. H: Microrill development in silt drape at edge of a sand blow. I: Post-depositional erosion of sand blow and silt drape to form parabolic microdunes and ripples only 2 mo after formation.

Figure 41: Figure 2 from Quigley et al. (2013) showing ejecta within Patch A for CES.

Figure 42: Ground photographs showing ejecta at the property with Patch A (photograph date: 22 June 2011).

Contents of this figure cannot be shared as doing so is restricted by a Non-Disclosure Agreement.

Figure 43: LDAT inspection notes for the property with Patch A (inspection date: Oct 2010).

Contents of this figure cannot be shared as doing so is restricted by a Non-Disclosure Agreement.

Figure 44: LDAT inspection notes for the property with Patch A (inspection date: 22 June 2011).

Figure 45: PGA for Sep-10 EQ (st. dev. = 0.300-0.325 ln units).

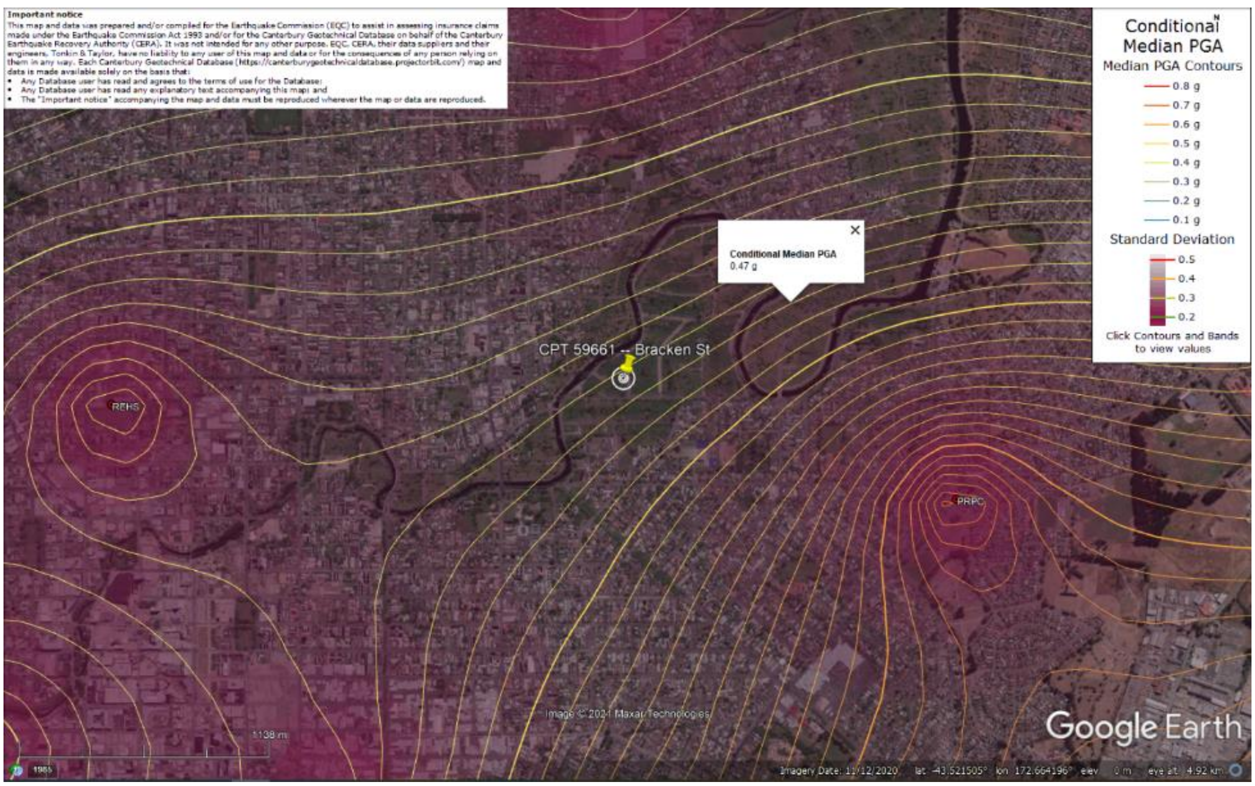

Figure 46: PGA for Feb-11 EQ (st. dev. = 0.325-0.350 ln units).

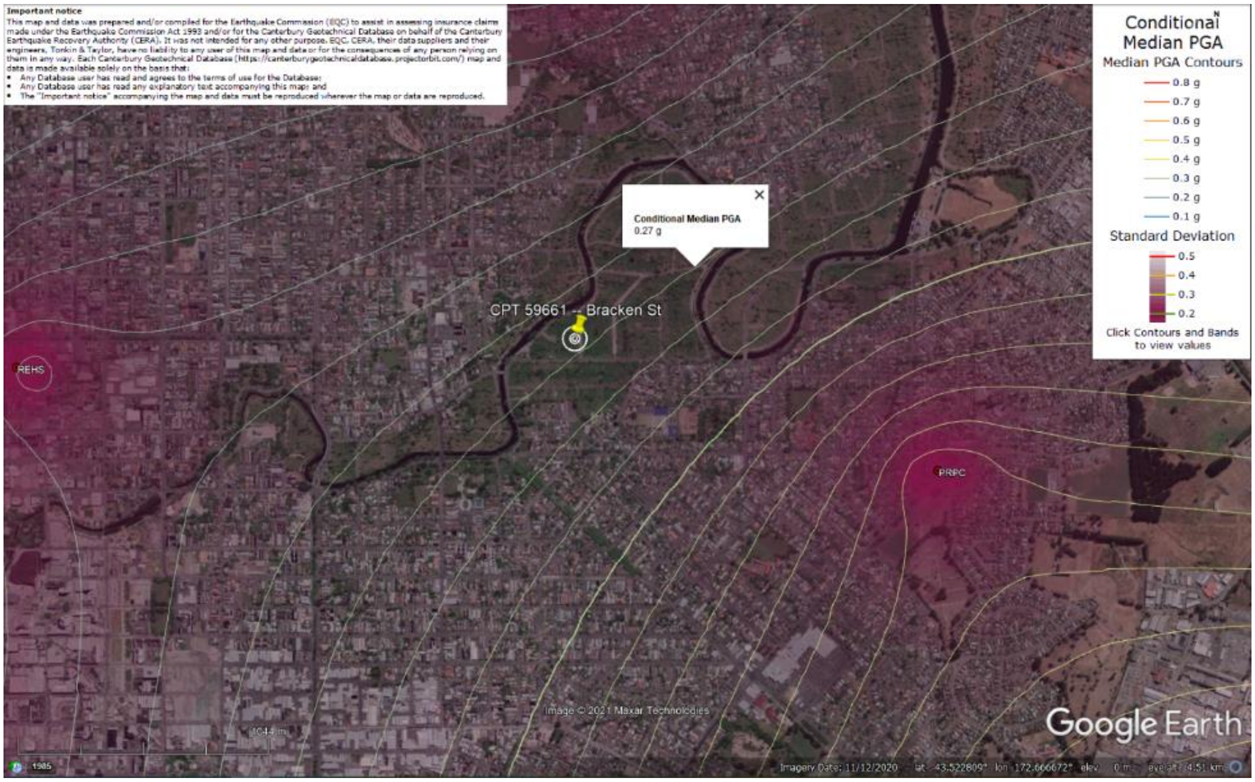

Figure 47: PGA for Jun-11 EQ (st. dev. = 0.350-0.375 ln units).

Figure 48: PGA for Dec-11 EQ (st. dev. = 0.350-0375 ln units).

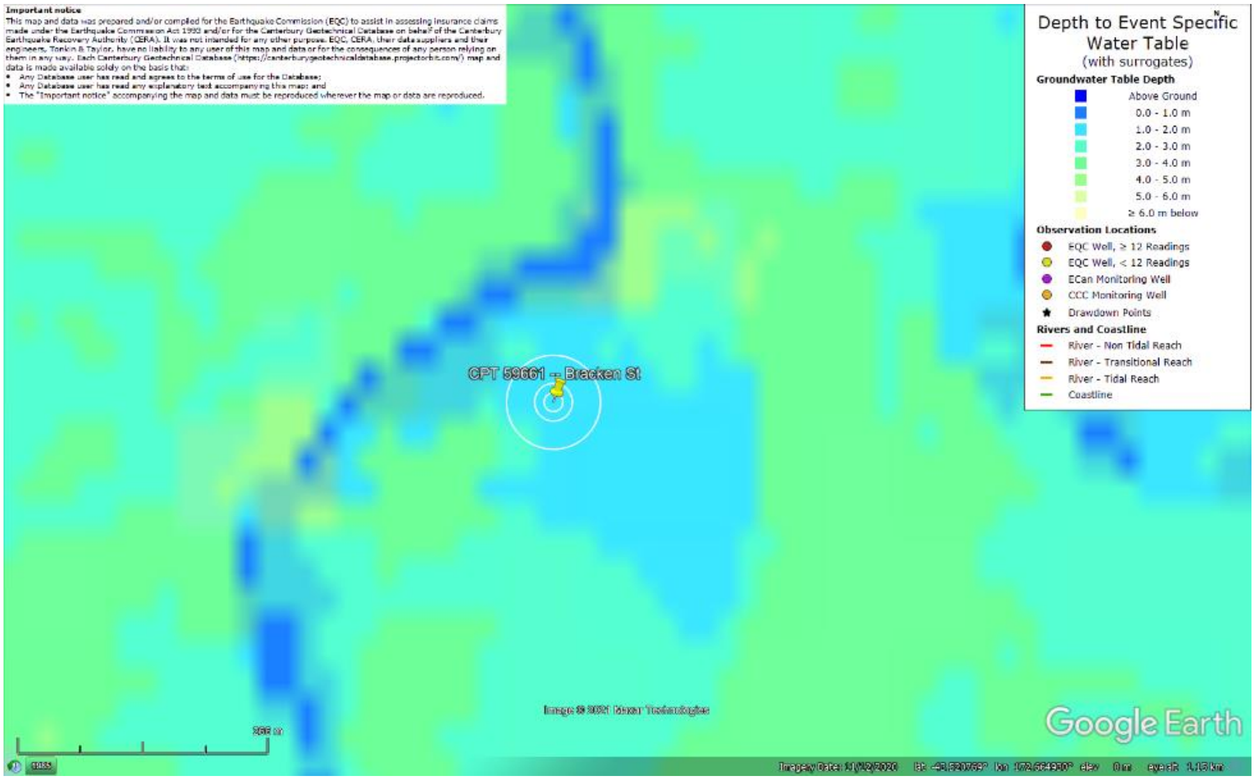

Figure 49: Depth to groundwater table for Sep-10 EQ.

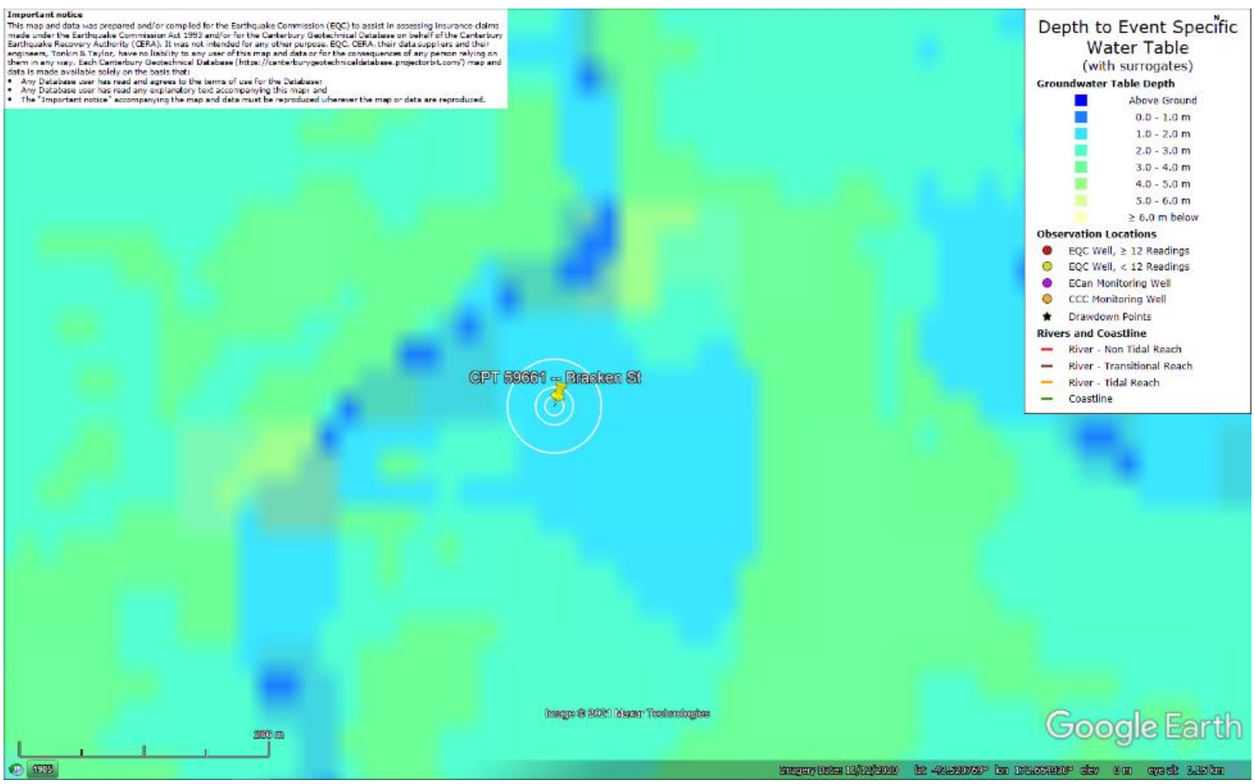

Figure 50: Depth to groundwater table for Feb-11 EQ.

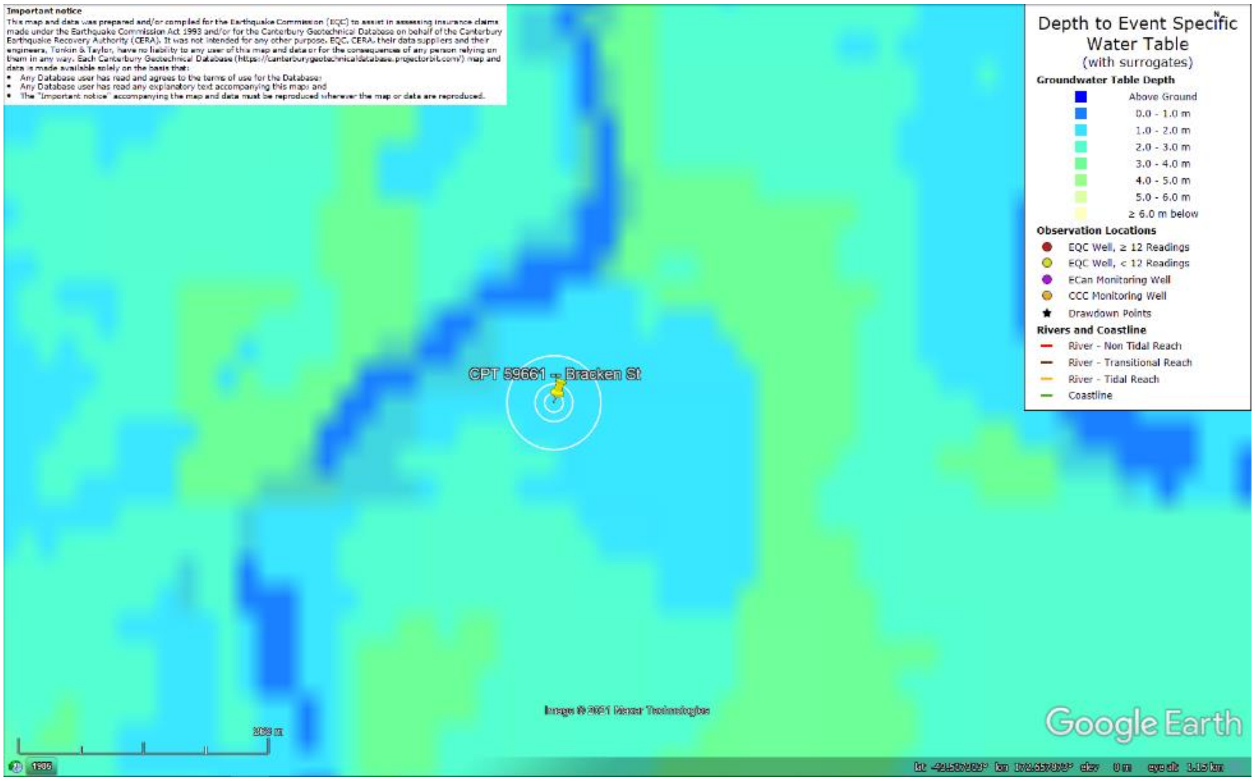

Figure 51: Depth to groundwater table for Jun-11 EQ.

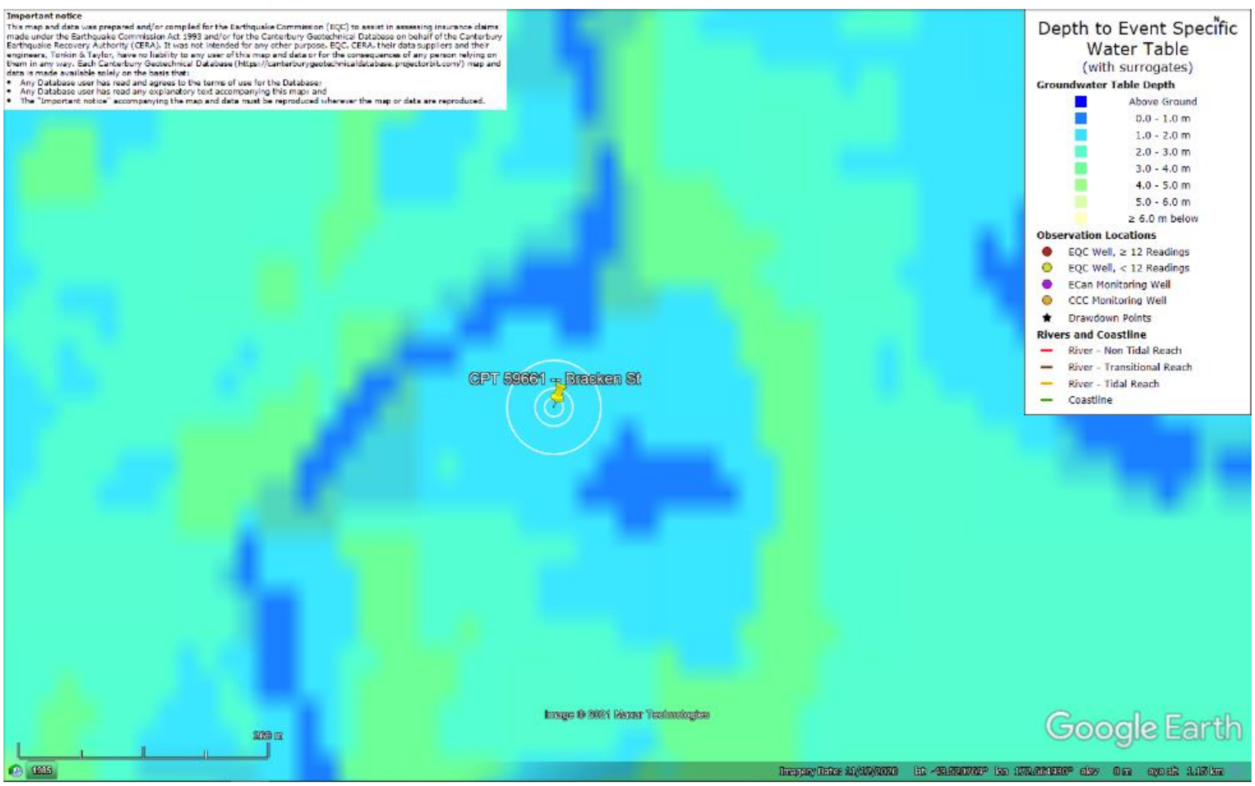

Figure 52: Depth to groundwater table for Dec-11 EQ.

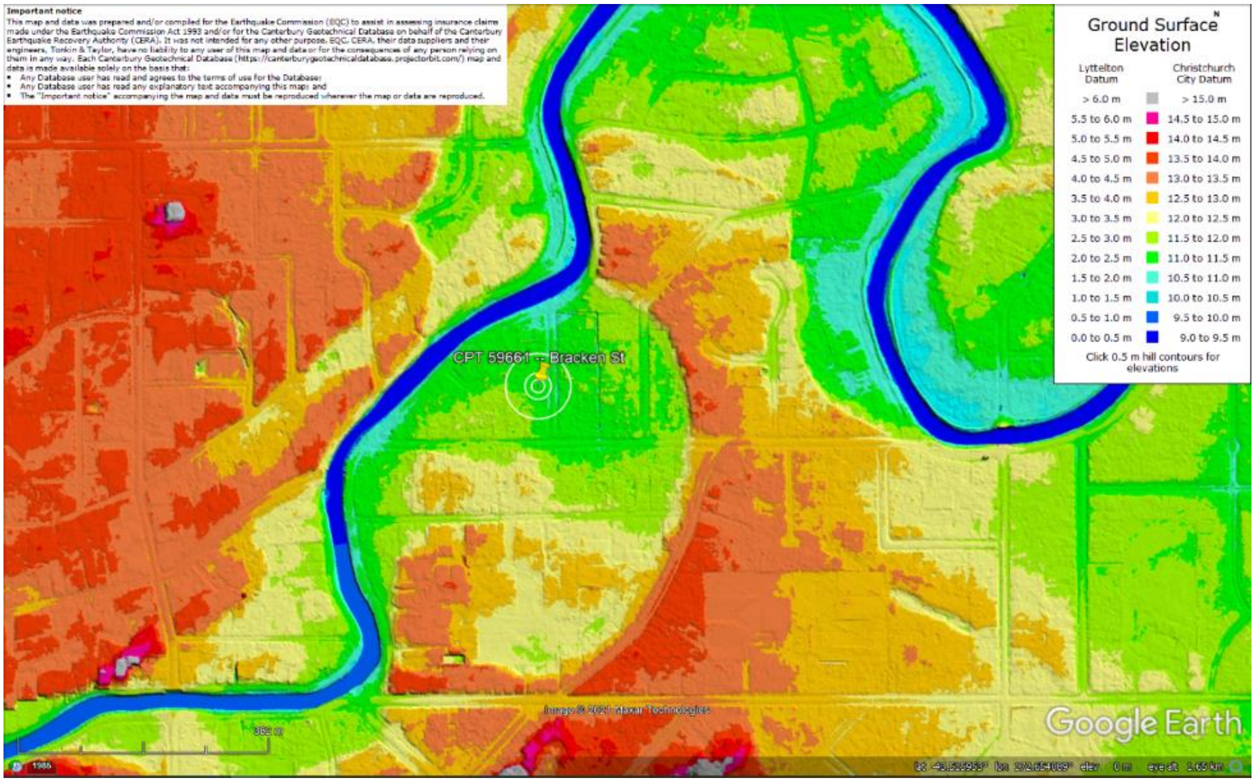

Figure 53: Ground surface elevation according to the Sep-11 LiDAR survey.

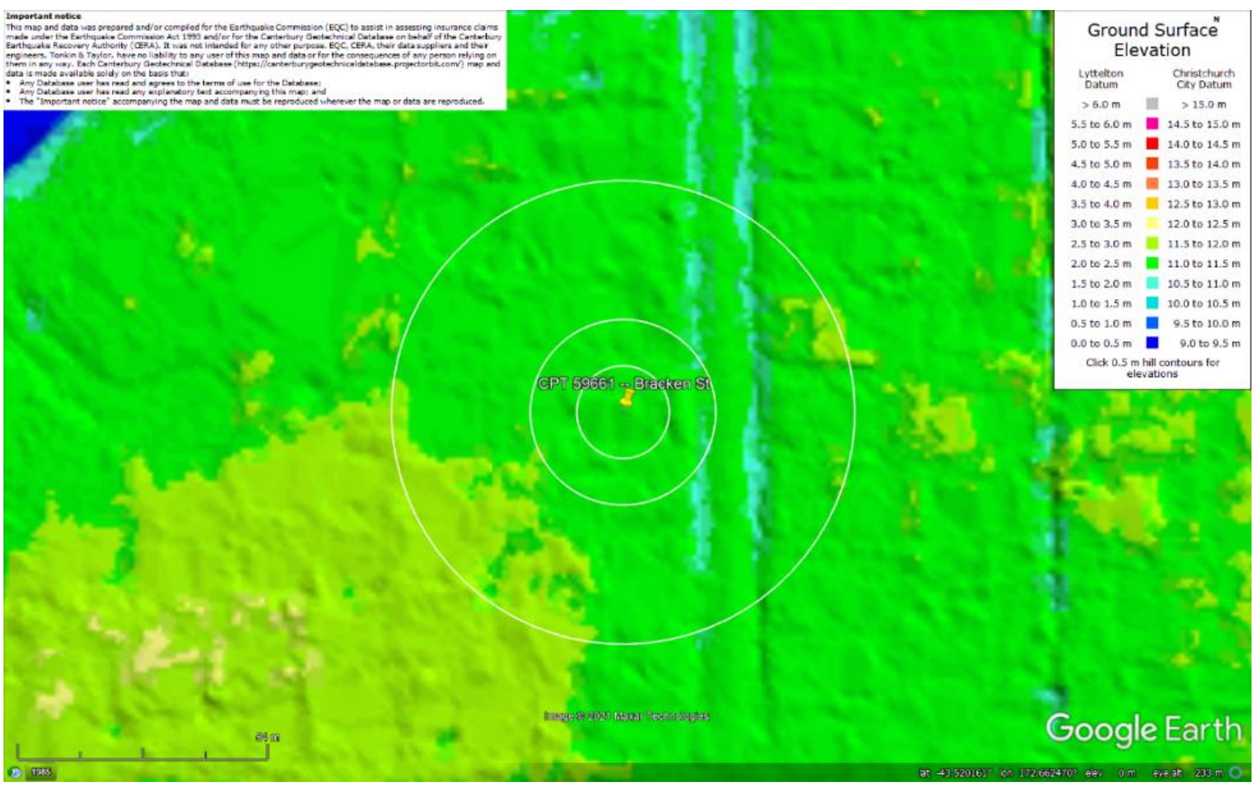

Figure 54: Ground surface elevation according to the Sep-11 LiDAR survey (enlarged).

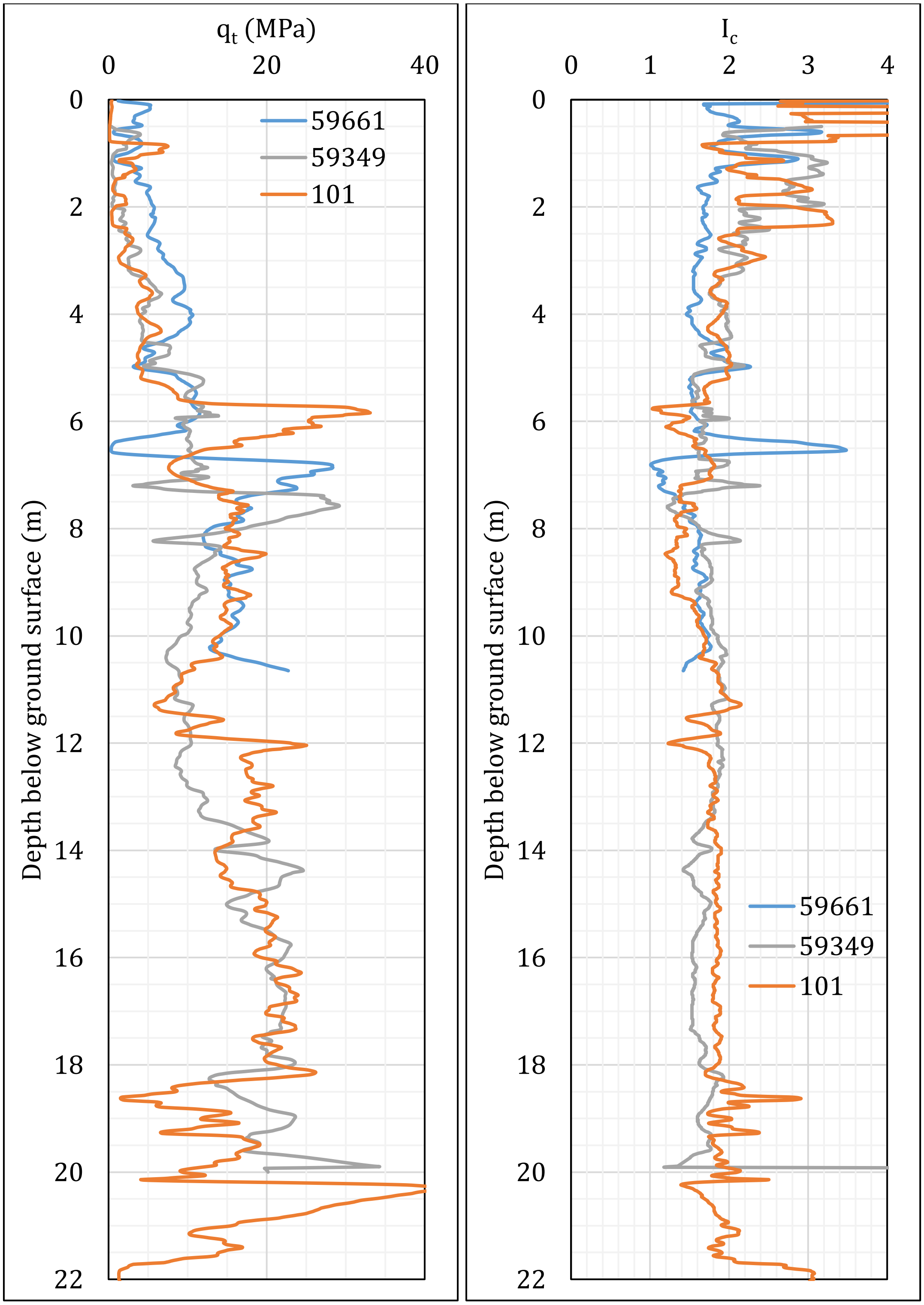

Figure 55: q_t and I_c profiles.

Note 6: The selection of CPTs for the area considered for settlement assessment (Figure 1) is based on the proximity of the CPTs to the considered areas. In accordance with that, the following table shows CPTs that were used for the volumetric settlement analysis in *Cliq v.3.0.3.2*, a CPT soil liquefaction software developed by GeoLogismiki. (The average volumetric settlements were reported in Table 8.)

Table 12: CPT profiles used in volumetric settlement analysis for areas selected for settlement assessment.

CPT ID No.	Patch A (50-m buffer)
59661 (57380)	✓
101	
59349 (61785)	

Notes: CPT 59661 was conducted on 18 Sep 2015, after the building was removed from the property; CPT 101 (~235 m to the SW from the center of the site) and CPT 59349 (~190 m to the NE from the center of the site) were the nearest CPTs with a 20-m penetration depth and were used to estimate the average volumetric settlement for a depth range from 10.7 m to 20 m.

Table 13: CPT-based results.

		CPT ID			
EQ Event	Parameter	59661	101	59349	$\Delta_{10.7m\text{-}20m}$
Sep-10	S_{V1D} (mm)	22	66	36	7
	LSN	6	15	8	1
	LPI	1	2	0	0
	LPI_{ish}	0	0	0	--
	$D_{FS<1}$ (m)	undet.	2.42	2.96	--
Feb-11	S_{V1D} (mm)	97	146	171	42
	LSN	29	29	32	4
	LPI	14	20	20	3
	LPI_{ish}	13	14	15	--
	$D_{FS<1}$ (m)	1.52	1.77	2.03	--
Jun-11	S_{V1D} (mm)	36	88	59	8
	LSN	11	21	15	1
	LPI	1	6	2	0
	LPI_{ish}	0	1	1	--
	$D_{FS<1}$ (m)	2.20	1.77	2.03	--
Dec-11	S_{V1D} (mm)	29	78	48	5
	LSN	8	19	13	1
	LPI	1	4	2	0
	LPI_{ish}	0	1	0	--
	$D_{FS<1}$ (m)	4.62	2.38	2.03	--

Notes: $D_{FS<1}$ = Depth to the first liquefiable layer (FS_L<1) that is at least 200-mm thick, as determined by the Boulanger and Idriss (2016) liquefaction-triggering procedure (P_L=50%, C_{FC}=0.13, and $I_{c,cutoff}$ =2.6), and exported from *Cliq v.3.0.3.2*; undet. = the specified soil layer was not detected; $\Delta_{10.7m\text{-}20m}$ indicates the amount of S_{V1D}, LSN, and LPI that could be added to CPT 59661 for a depth range from 10.7 m to 20 m due to its shallow penetration depth.

Note 7: Based on the borehole log BH 59898 (~90 m to the SE from the center of the site), the groundwater table is at a depth of 1.9 m below the ground surface (BGS). According to the borehole log BH 59894 (~190 m to the NE from the center of the site) and CPT 59661, the soil profile consists of (1) (sandy) silt, ML, to a depth of ~2.5 m, (2) fine to medium sand, SP, to a depth of ~4.5 m, (3) sandy silt, ML, to a depth of ~5 m, fine to medium sand, SP, to a depth of ~6.3 m, silt, ML, to a depth of ~6.8 m, fine to coarse sand, SP/SW, to a depth of ~10.5 m (the end of CPT). The BH 59894 and BH 59898 suggest that the SP layer extends to a depth of ~20 m. It is estimated that the change from the Springston formation to the Christchurch formation occurs at a depth of ~7 m BGS.

Note 8: The ejecta-induced free-field settlement provided in Table 11 is an areal average settlement due to ejecta, which is based on the total settlement assessment area, A_T (provided in Table 9 and repeated in Table 14). However, the considered area was not always covered completely with ejecta; thus, it is important to provide the localized ejecta-induced settlement, too. The localized settlement due to ejecta is estimated using photographic evidence only as

$$S_{E,P\_localized} = \frac{V_E}{A_E}$$

where V_E is the total volume of ejecta within A_T and A_E is the total coverage area of ejecta within A_T. Please note that the areal ejecta-induced settlement provided in Table 14 as S_{E,P_areal} is the same as $S_{E,P}$ in Table 11, which was estimated as

$$S_{E,P\_areal} = S_{E,P} = \frac{V_E}{A_T}$$

where V_E is the total volume of ejecta within A_T and A_T is the total settlement assessment area.

Table 14: Areal and localized ejecta-induced settlement estimates for Patch A based on photographic evidence.

Earthquake Event	A_T (m²)	A_E (m²)	V_E (m³)	S_{E,P_areal} (mm)	$S_{E,P\_localized}$ (mm)
Sep-10	103	60.3	3.3-5.3	40±10	70±15
Feb-11	103	68.2	6.4-8.8	75±10	110±15
Jun-11	103	44.4	2.1-3.5	25±5	60±15
Dec-11	103	27.6	1.4-2.1	15±5	65±10

Notes: S_{E,P_areal} = $S_{E,P}$ reported in Table 11 = areal ejecta-induced settlement; $S_{E,P\_localized}$ = localized ejecta-induced settlement; A_T = total settlement assessment area; V_E = total volume of ejecta within A_T; A_E = total area of ejecta within A_T; The estimates of both areal and localized ejecta-induced settlement are rounded to the nearest 5; Final plus/minus values are also rounded to the nearest 5.

Summary 2:

The best estimate of the localized ejecta-induced free-field ground settlement at the Bracken St site for the SEP 2010, FEB 2011, JUN 2011, and DEC 2011 earthquake is 70±15 mm, 110±15 mm, 60±15 mm, and 65±10 mm, respectively.